Progress In Electromagnetics Research, Vol. 114, 333–352, 2011

A HIGH ORDER INTEGRAL SPM FOR THE CONDUCTING ROUGH SURFACE SCATTERING WITH THE TAPERED WAVE INCIDENCE-TE CASE

L.-X. Guo, Y. Liang, J. Li, and Z.-S. Wu

School of Science, Xidian University
No. 2, Taibai Road, Xi'an, Shaanxi, China

Abstract—Based on the Helmholtz integral equation and series expansion theory, a high order integral small perturbation method (HISPM) for studying electromagnetic wave scattering from the finite conducting rough surface with tapered transverse electric (TE) wave incidence is presented. The high order scattering coefficients are obtained by the series expansion, the validity and accuracy of HISPM is verified through numerical evaluation with classical small perturbation method (CSPM) and the method of moments (MOM) By comparing with CSPM for the infinite rough surface case with plane wave incidence, the presented HISPM can greatly reduce the edge diffraction effect. HISPM also shows advantages in the memory requirement and computational time, especially in calculating scattering coefficients with low grazing angle incidence. Numerical examples are given to show that with the increasing of the length of the rough surface, the memory requirements and the computation time of HISPM are dramatically reduced compared to those of MOM.

1. INTRODUCTION

Electromagnetic (EM) waves scattering from the randomly rough surface has been an important research subject over the past several decades owing to its important applications in many domains, such as remote sensing, oceanography, communications, material science, electromagnetics and applied optics, etc. As a whole, methods in studying the rough surface scattering can be categorized into two groups: (1) approximate and analytical methods, and (2) numerical methods. The approximate methods mainly includes: the small-perturbation method (SPM) [1–4] for small-scale roughness rough

Received 16 January 2011, Accepted 21 February 2011, Scheduled 3 March 2011
Corresponding author: Li-Xin Guo (lxguo@mail.xidian.edu.cn).

surface, the Kirchhoff or tangent plane approximation (KA) [5–7] for large-scale roughness surface, the physical optics (PO) method, the two-scale method (TSM) [8] that combing the SPM and the KA, employing the SPM on nearly flat facets with a small-scale roughness, and then averaging the scattering contributions on the tilted large-scale roughness component that can be analyzed by the KA. In recent years, some other approximate methods, such as the phase perturbation method (PPM) [9], the rayleigh method [10], the extended boundary condition method [11], small-slope approximation (SSA), and the unified perturbation method (UPM), etc, are also presented for rough surface scattering. In the other hand, some numerical approaches, such as the method of moments (MOM) [12–15], the finite difference time domain (FDTD) method [16–18], the finite element method (FEM) [19], the fast multipole method (FMM) [20], the forward-backward method (FBM) [21] and the SMCG/PBTG method [22], etc. have been applied to the problem of EM scattering from rough surface.

This paper is devoted to the scattering from the slightly rough surface, where both the rms height h and correlation length l are smaller than the incident wavelength. As we have already known, the SPM has been proved to be a very effective method for such a problem, many very valuable works have been done during the past few decades. The small-perturbation theory was firstly presented by Rice [1] for researching the reflection of electromagnetic waves from the surface that is slightly rough. Then, the SPM based on Rayleigh approximation is given by Beckmann et al. [7], the diagram method was presented by Bass and Fuks [23] in studying the perturbation method for rough surface scattering. Thorsos and Jackson [24] examined the validity of perturbation approximation for acoustic scattering from one-dimensional perfectly conducting rough surface by comparing with results obtained by solving an integral equation, it is noticeable that, the tapered plane wave was firstly applied in the scattering calculation. Soto-Crespo et al. studied the validity of small perturbation method derived from the Rayleigh hypothesis and extinction theorem respectively in [25], in which they compared results of SPM with those obtained by using the Kirchhoff approximation, as well as the exact numerical method. The range of validity of perturbation theory was also discussed by Kim and Stoddart [26].

Based on the extension of the diagram method, Ishimaru et al. discussed the first-order modified perturbation theory with the help of rough surface Green's function in [27], where scattering from one-dimensional rough surfaces with a Dirichlet boundary condition is studied. And in [27], Ishimaru et al. obtained the coherent Green's function from the smoothed Dyson's equation using a spatial Fourier

transform, and obtained the mutual coherence function for the Green's function by the first-order iteration of the smoothing approximation applied to the Bethe-Salpeter equation. Guérin and Sentenac applied the second-order perturbation theory in investigating scattering from heterogeneous rough surfaces [28]. Later, the effects of multiple scattering due to the surface roughness are incorporated systematically into the solutions of Ishimaru et al. [27] by Brelet and Bourlier [29], applying an effective surface impedance for a one-dimensional perfectly conducting Gaussian rough surface, to compare the resultant bistatic scattering coefficients with the first- and second-order conventional small perturbation method.

In fact, not only the Green function, but also the field can be expanded on the unperturbed surface. In calculation of the radar scattering coefficient, except the Green function itself, the electromagnetic field value is also very important. Therefore, it is naturally that the field, not only the Green function, should be concerned directly, and this is also what we will actually do in the following context. Furthermore, the length of the surface which we investigate scattering from often plays an important role in determining the width of the specular peak which is brought in by the coherent scattering. Although the series expansion of the field is used in the classical SPM (CSPM) [1, 2] which are very valuable, but the infinite length rough surface is concerned, resulting in the lack of investigation on the width of specular peak. What's more, CSPM has the following two drawbacks, i.e., coherent and incoherent scattering are discussed separately, and only the low order cases are discussed. Tsang [3] and Johnson et al. [4] extended the CSPM to the second and third order, separately, and obtained the analytical expressions of the scattering coefficient for the infinite length rough surface, it is very important and luminous. Based on the previous important ideas about the SPM, especially the Tsang's and Johnson's work, and considering the length of the rough surface is infinite, in this paper, the series expansion of the field on the finite length rough surface is applied, and the expression of arbitrary high order scattering coefficient is presented where coherent and incoherent scattering is considered simultaneously (in Tsang's and Johnson's work, the coherent and incoherent scattering is considered separately). As the model studied is the finite length surface, the scattering characteristic of the specular peak can be investigated. It is noted that, in this paper, Thorsos tapered wave is applied to avoid the so called edge diffraction effect. It is also addressed that, in most of the previous research about the SPM, the spectral density function of the surface height is needed in the calculation of the analytical scattering coefficients including the Tsang's and Johnson's work, etc.,

but in our present work, only the surface height profile is required, the treatment and the expression of the scattering coefficients may be call as 'semi-analytical' (intermediate in some respects between the analytical and the numerical methods), due to the calculating process is a little similar with that of some numerical methods (such as the MOM), firstly, we obtain several discretized location information, that is, the discretized abscissa and discretized height of the rough surface, then, basing the location information, through the integral operation, some unknown quantities, such as the zero-order, first-order, second-order, third-order, $\cdots$, and till nth-order partial derivative of the zero-order, first-order, second-order, third-order, $\cdots$, and till nth-order field are obtained, something like the obtained unknown current in the MOM, next, substitute the location information and the unknown quantities into the expression of the scattering coefficients, also through the integral operation, the final results are obtained, we also temporarily named this 'semi-analytical' high order SPM as the 'high order integral SPM (HISPM)'. The validity of our method is verified by comparing with the classical SPM, as well as MOM which is proved to be an accurate numerical method in calculating the wave scattering coefficient from the rough surface. Considering the fact that the permittivity and conductive lossiness of sea water at microwave frequencies are very high, the PEC (perfect electric conductor) model is a suitable model for EM waves scattering from ocean surface. Therefore, our study will be useful for remote sensing of ocean, especially when the transmitter is close to sea surface with low wind speed above it.

The organization of this paper is as follows. In Section 2, the integral equations based on the Green theorem and the Ewald-Oseen extinction theorem [30] for the rough surface scattering are presented. In Section 3, for TE case, based the series expansion of the field, the formulation of higher-order integral SPM (HISPM) is presented, and the normalized high order far-field scattering coefficient is obtained. In Section 4, numerical results of HISPM, as well as comparisons with the classical SPM and MOM and detailed discussion are given. Finally, concluding remarks are addressed in Section 5.

2. INTEGRAL EQUATIONS FOR ROUGH SURFACE SCATTERING

Consider an electromagnetic wave φ_i (as shown in Fig. 1) impinging upon a one dimensional rough surface S, where the surface height profile is denoted by $z = f(x)$ with the spectral density function $W(k)$. $W(k)$ is an inversion Fourier transform of the surface height correlation

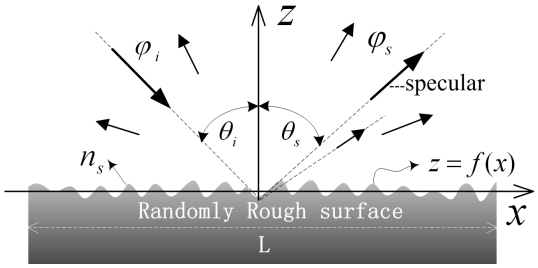

Figure 1. The sketch for wave scattering by a randomly rough surface.

function $C(f(x))$ that is, $W(k) = F^{-1}[C(f(x))]$. The scattered field is denoted by φ_s. The generation of the surface profile can be realized by Monte Carlo simulations [14]. Let us consider the contour integral over the surface, which is composed of the surface boundary S and the half-circle of radius extending to infinity. Applying the Green's second theorem and the divergence theorem [14], the following equation is obtained

$$\iint_V \left[\varphi\nabla^2 g(\mathbf{r},\mathbf{r}') - g(\mathbf{r},\mathbf{r}')\nabla^2\varphi\right] dv = \oint_S \left[\varphi\frac{\partial}{\partial n}g(\mathbf{r},\mathbf{r}') - g(\mathbf{r},\mathbf{r}')\frac{\partial}{\partial n}\varphi\right] ds$$
$$= \int_S \left[\varphi\frac{\partial}{\partial n_s}g(\mathbf{r},\mathbf{r}') - g(\mathbf{r},\mathbf{r}')\frac{\partial}{\partial n_s}\varphi\right] ds$$
$$+ \int_\infty \left[\varphi\frac{\partial}{\partial n_\infty}g(\mathbf{r},\mathbf{r}') - g(\mathbf{r},\mathbf{r}')\frac{\partial}{\partial n_\infty}\varphi\right] ds \quad (1)$$

where $\hat{\mathbf{n}}_s$ is the unit normal vector on the boundary of the surface S, $\hat{\mathbf{n}}_\infty$ is the unit normal vector of the surface at infinity. The second integral term on the right-hand side of above equation denotes the incident field at infinity, that is

$$\varphi_i(\mathbf{r}') = \int_\infty \left[\varphi\frac{\partial}{\partial n_\infty}g(\mathbf{r},\mathbf{r}') - g(\mathbf{r},\mathbf{r}')\frac{\partial}{\partial n_\infty}\varphi\right] ds \quad (2)$$

where $g(\mathbf{r},\mathbf{r}')$ is the dyadic Green function. The wave function φ and the dyadic Green function $g(\mathbf{r},\mathbf{r}')$ satisfy the following two equations

$$\nabla^2\varphi = -k^2\varphi, \quad \nabla^2 g(\mathbf{r},\mathbf{r}') = \delta(\mathbf{r}-\mathbf{r}') - k^2 g(\mathbf{r},\mathbf{r}') \quad (3)$$

Then, the left-hand side of (1) can be written as

$$\iint_V \left[\varphi\nabla^2 g(\mathbf{r},\mathbf{r}') - g(\mathbf{r},\mathbf{r}')\nabla^2\varphi\right] dv = -\iint_V dr\delta(\mathbf{r}-\mathbf{r}')\varphi(\mathbf{r}) \quad (4)$$

where $\mathbf{r}' = (x', z')$ is the observation point location vector far away from the rough surface. Therefore, according to the Ewald-Oseen extinction theorem (or extended boundary condition) [30], the scattered field in the region above the rough surface ($z' > \max f(x)$) and the incident field below the rough surface ($z' < \min f(x)$) reduce to

$$\begin{cases} \varphi_s(r') = \displaystyle\int_S \left[\varphi \frac{\partial}{\partial n_s} g\left(\mathbf{r}, \mathbf{r}'\right) - g\left(\mathbf{r}, \mathbf{r}'\right) \frac{\partial}{\partial n_s}\varphi\right] ds \quad (z' > \max f(x)) \\ \varphi_i(r') = -\displaystyle\int_S \left[\varphi \frac{\partial}{\partial n_s} g\left(\mathbf{r}, \mathbf{r}'\right) - g\left(\mathbf{r}, \mathbf{r}'\right) \frac{\partial}{\partial n_s}\varphi\right] ds \; (z' < \min f(x)) \end{cases} \tag{5}$$

where the dyadic Green function $g(\mathbf{r}, \mathbf{r}')$ equals $H_0^{(1)}(\mathbf{r}, \mathbf{r}')$, i.e., the zeroth-order Hankel function of the first kind. The first upper equation in (5) is called as the Helmholtz integral equation for scattered filed, while the second one corresponds to that of incident filed.

3. THE FORMULATION OF HIGHER-ORDER INTEGRAL SPM

When the slightly rough surface is concerned, the rms height of the surface is far smaller than the incident wavelength [3]. The field at the surface is related with the profile of the scattering surface, i.e., the EM field is function of the surface height. Therefore, according to the series expansion theory which is valid when the variable (i.e., the height of the profile) is small the field on the surface can be expanded as a Taylor series about the field on the unperturbed surface (mean plane surface)

$$\begin{aligned} \varphi|_{z=f(x)} &= \sum_n \frac{f^n}{n!} \frac{\partial^n}{\partial z^n} \varphi|_{z=0} \\ &= \varphi|_{z=0} + f \frac{\partial}{\partial z}\varphi\bigg|_{z=0} + \frac{f^2}{2!} \frac{\partial}{\partial z} \frac{\partial}{\partial z}\varphi\bigg|_{z=0} \\ &\quad + \frac{f^3}{3!} \frac{\partial}{\partial z} \frac{\partial}{\partial z} \frac{\partial}{\partial z}\varphi\bigg|_{z=0} + \cdots + \frac{f^N}{N!} \frac{\partial^N}{\partial z^N} \varphi|_{z=0} \end{aligned} \tag{6}$$

where $\varphi|_{z=0}$ is the total field at the unperturbed surface. Scattering field can be expressed as the sum of the zero-order, the first-order, ..., and nth-order scattered field as following

$$\varphi_s = \varphi_0^s + \varphi_1^s + \varphi_2^s + \varphi_3^s \cdots + \varphi_n^s \tag{7}$$

where φ_0^s denotes the specular component of the scattered field, which can be obtained by the incident field. By applying Dirichlet boundary condition for HH polarization (TE case), under this condition, φ_i and

φ_s denote the electric field component of the incident and scattered electromagnetic waves, respectively, that is, $\varphi_i = E_i\hat{\mathbf{y}}$, $\varphi_s = E_s\hat{\mathbf{y}}$, we obtain

$$\begin{aligned}
&\varphi_i|_{z=0} + \varphi_0^s|_{z=0} + \varphi_1^s|_{z=0} + \varphi_2^s|_{z=0} + \cdots + \varphi_n^s|_{z=0} \\
&+f\,\frac{\partial}{\partial z}\left(\varphi_i + \varphi_0^s + \varphi_1^s + \varphi_2^s + \cdots + \varphi_{n-1}^s\right)\Big|_{z=0} \\
&+\frac{f^2}{2!}\frac{\partial}{\partial z}\frac{\partial}{\partial z}\left(\varphi_i + \varphi_0^s + \varphi_1^s + \varphi_2^s \cdots + \varphi_{n-2}^s\right)\Big|_{z=0} \\
&+\frac{f^3}{3!}\frac{\partial}{\partial z}\frac{\partial}{\partial z}\frac{\partial}{\partial z}\left(\varphi_i + \varphi_0^s + \varphi_1^s + \varphi_2^s \cdots + \varphi_{n-3}^s\right)\Big|_{z=0} + \cdots \\
&+\frac{f^n}{n!}\underbrace{\frac{\partial}{\partial z}\frac{\partial}{\partial z}\cdots\frac{\partial}{\partial z}}_{n}\left(\varphi_i + \varphi_0^s\right)\Bigg|_{z=0} = 0
\end{aligned} \tag{8}$$

Derivative terms with the same order on both side of the above equation have the same value, therefore the first-order, second-order, third-order, ..., nth-order boundary relationships can be obtained as following

$$\varphi_1^s|_{z=0} = -\left(f\frac{\partial}{\partial z}\,\varphi_i|_{z=0} + f\frac{\partial}{\partial z}\,\varphi_0^s|_{z=0}\right) \tag{9a}$$

$$\varphi_2^s|_{z=0} = -f\frac{\partial}{\partial z}\,\varphi_1^s|_{z=0} - \frac{f^2}{2!}\frac{\partial}{\partial z}\frac{\partial}{\partial z}\left(\varphi_0^s + \varphi_i\right)\Big|_{z=0} \tag{9b}$$

$$\begin{aligned}
\varphi_3^s|_{z=0} = &-f\frac{\partial}{\partial z}\,\varphi_2^s|_{z=0} - \frac{f^2}{2!}\frac{\partial}{\partial z}\frac{\partial}{\partial z}\varphi_1^s\Big|_{z=0} \\
&- \frac{f^3}{3!}\left(\frac{\partial}{\partial z}\frac{\partial}{\partial z}\frac{\partial}{\partial z}\varphi_i + \frac{\partial}{\partial z}\frac{\partial}{\partial z}\frac{\partial}{\partial z}\varphi_0^s\right)\Big|_{z=0}
\end{aligned} \tag{9c}$$

$$\cdots$$

$$\begin{aligned}
\varphi_n^s|_{z=0} = &-f\frac{\partial}{\partial z}\,\varphi_{n-1}^s\big|_{z=0} - \frac{f^2}{2}\frac{\partial}{\partial z}\frac{\partial}{\partial z}\varphi_{n-2}^s\Big|_{z=0} - \cdots \\
&- \frac{f^n}{n!}\left(\underbrace{\frac{\partial}{\partial z}\frac{\partial}{\partial z}\cdots\frac{\partial}{\partial z}}_{n}\varphi_i + \underbrace{\frac{\partial}{\partial z}\frac{\partial}{\partial z}\cdots\frac{\partial}{\partial z}}_{n}\varphi_0^s\right)\Bigg|_{z=0}
\end{aligned} \tag{9n}$$

In the spectral domain, the first-order to the nth-order scattered field can be expressed as the following equations

$$\varphi_m\left(\mathbf{r}'\right) = \int_{-\infty}^{\infty} dk_x A_m\left(k_x\right) \exp\left(i\left(k_x x' + k_z z'\right)\right), \quad (m = 1 \sim n) \tag{10}$$

So the following relationships are obtained on the surface interface, i.e.,

$$\varphi_m\left(\mathbf{r}\right)\big|_{z=0} = \int_{-\infty}^{\infty} dk_x A_m\left(k_x\right) \exp\left(ik_x x\right), \quad (m = 1 \sim n) \tag{11}$$

$$\frac{\partial^n}{\partial z^n}\varphi_m\left(\mathbf{r}\right)\bigg|_{z=0} = i^n \int_{-\infty}^{\infty} dk_x k_z^n A_m\left(k_x\right) \exp\left(ik_x x\right), \ (m = 1 \sim n) \tag{12}$$

By performing Fourier transform of (11), the amplitudes of $A_1(k_x)$, $A_2(k_x)$, $\cdots$, $A_n(k_x)$ are determined. Then these amplitudes are substituted into (12), and inversion Fourier transform is used subsequently. Therefore the partial derivative terms $(\partial^n/\partial z^n)\varphi_m(\mathbf{r})|_{z=0}$, $(m = 1 \sim n)$ can be obtained. These partial derivative terms are needed in the calculation of (9a)–(9n), of which the first three orders about the incident field and zeroth-order scattered field can be obtained according to the incident field. As the field discussed is above the unperturbed surface, the half-space dyadic Green's function should be considered in (5). It can be obtained through the sum of free-space Green's function and the one associated with an image source as following

$$g_R(\mathbf{r}, \mathbf{r}') = g(\mathbf{r}, \mathbf{r}') + Rg_I(\mathbf{r}, \mathbf{r}') \tag{13}$$

where $g_I(\mathbf{r}, \mathbf{r}') = g(\mathbf{r}, \mathbf{r}' - 2\hat{\mathbf{z}}(\hat{\mathbf{z}} \cdot \mathbf{r}'))$, R denotes the reflection coefficient that is related with the permittivity ε and permeability μ. For conducting surface R equals -1, thus in the unperturbed surface, the half-space Green's function is zero, that is, $g_R(\mathbf{r}, \mathbf{r}')|_{S_m} = 0$. Therefore, the scattered field in (5) is converted into the following equation

$$\varphi_s(\mathbf{r}') = -\int_s ds \varphi_s(\mathbf{r}) \frac{\partial}{\partial n_s} g_R(\mathbf{r}, \mathbf{r}') \tag{14}$$

where $\varphi_s(\mathbf{r})$ is the scattered field at the unperturbed surface. Thus the first-order, second-order, third-order, $\cdots$, and till nth-order scattered field can be obtained through integrating over the unperturbed surface S_m as following

$$\begin{aligned} \varphi_1^s(\mathbf{r}') \ = \ & -\int_{S_m} dS_m \frac{\partial}{\partial n_s} g_R(\mathbf{r}, \mathbf{r}') \\ & \cdot \left(\varphi_i|_{z=0} + f\frac{\partial}{\partial z}\varphi_i|_{z=0} + f\frac{\partial}{\partial z}\varphi_0^s|_{z=0}\right) \end{aligned} \tag{15a}$$

$$\varphi_2^s(\mathbf{r}') = -\int_{S_m} dS_m \frac{\partial}{\partial n_s} g_R(\mathbf{r},\mathbf{r}') \cdot \left(\varphi_i|_{z=0} + f\frac{\partial}{\partial z}(\varphi_i + \varphi_0^s + \varphi_1^s)|_{z=0} + \frac{f^2}{2!}\frac{\partial}{\partial z}\frac{\partial}{\partial z}(\varphi_0^s + \varphi_i)|_{z=0} \right) \tag{15b}$$

$$\varphi_3^s(\mathbf{r}') = -\int_{S_m} dS_m \frac{\partial}{\partial n_s} g_R(\mathbf{r},\mathbf{r}') \begin{pmatrix} \varphi_i|_{z=0} + f\frac{\partial}{\partial z}(\varphi_i + \varphi_0^s + \varphi_1^s + \varphi_2^s)|_{z=0} \\ + \frac{f^2}{2!}\frac{\partial}{\partial z}\frac{\partial}{\partial z}(\varphi_0^s + \varphi_i + \varphi_1^s)|_{z=0} \\ + \frac{f^3}{3!}\frac{\partial}{\partial z}\frac{\partial}{\partial z}\frac{\partial}{\partial z}(\varphi_i + \varphi_0^s)|_{z=0} \end{pmatrix} \tag{15c}$$

$$\cdots$$

$$\varphi_n^s(\mathbf{r}') = -\int_{S_m} dS_m \frac{\partial}{\partial n_s} g_R(\mathbf{r},\mathbf{r}') \cdot \begin{pmatrix} \varphi_i|_{z=0} + f\frac{\partial}{\partial z}\left(\varphi_i + \varphi_0^s + \varphi_1^s + \varphi_2^s + \cdots + \varphi_{n-1}^s\right)\big|_{z=0} \\ + \frac{f^2}{2!}\frac{\partial}{\partial z}\frac{\partial}{\partial z}\left(\varphi_i + \varphi_0^s + \varphi_1^s + \varphi_2^s + \cdots + \varphi_{n-2}^s\right)\Big|_{z=0} \\ + \frac{f^3}{3!}\frac{\partial}{\partial z}\frac{\partial}{\partial z}\frac{\partial}{\partial z}\left(\varphi_i + \varphi_0^s + \varphi_1^s + \varphi_2^s + \cdots + \varphi_{n-3}^s\right)\Big|_{z=0} \\ + \cdots + \frac{f^n}{n!}\underbrace{\frac{\partial}{\partial z}\frac{\partial}{\partial z}\cdots\frac{\partial}{\partial z}}_{n}(\varphi_i + \varphi_0^s)\Big|_{z=0} \end{pmatrix} \tag{15n}$$

When the half-space dynamic Green's function is expanded at infinity and substituted into equations above, all the scattered fields can be written as

$$\varphi_1^s(\mathbf{r}') = -\frac{1}{\sqrt{2\pi kr'}}\exp(ikr')\exp(-i\pi/4)k\cos\theta_s\varphi_1^{Ns}(\theta_s) \tag{16a}$$

$$\varphi_2^s(\mathbf{r}') = -\frac{1}{\sqrt{2\pi kr'}}\exp(ikr')\exp(-i\pi/4)k\cos\theta_s\varphi_2^{Ns}(\theta_s) \tag{16b}$$

$$\varphi_3^s(\mathbf{r}') = -\frac{1}{\sqrt{2\pi kr'}}\exp(ikr')\exp(-i\pi/4)k\cos\theta_s\varphi_3^{Ns}(\theta_s) \tag{16c}$$

$$\cdots$$

$$\varphi_n^s(\mathbf{r}') = -\frac{1}{\sqrt{2\pi kr'}}\exp(ikr')\exp(-i\pi/4)k\cos\theta_s\varphi_n^{Ns}(\theta_s) \tag{16n}$$

$$\varphi_1^{Ns}(\theta_s)=\int_{-\frac{L}{2}}^{\frac{L}{2}} dx\left(\varphi_i|_{z=0}+f\frac{\partial}{\partial z}\varphi_i|_{z=0}+f\frac{\partial}{\partial z}\varphi_0^s|_{z=0}\right)\exp(-ik\sin\theta_s x) \tag{17a}$$

$$\begin{aligned}\varphi_2^{Ns}(\theta_s) \;=\; &\int_{-\frac{L}{2}}^{\frac{L}{2}} dx\left(\varphi_i|_{z=0}+f\frac{\partial}{\partial z}\left(\varphi_i+\varphi_0^s+\varphi_1^s\right)|_{z=0}\right.\\ &\left.+\frac{f^2}{2!}\frac{\partial}{\partial z}\frac{\partial}{\partial z}\left(\varphi_0^s+\varphi_i\right)\Big|_{z=0}\right)\exp\left(-ik\sin\theta_s x\right)\end{aligned} \tag{17b}$$

$$\varphi_3^{Ns}(\theta_s)=\int_{-\frac{L}{2}}^{\frac{L}{2}} dx\begin{pmatrix}\varphi_i|_{z=0}+f\frac{\partial}{\partial z}(\varphi_i+\varphi_0^s+\varphi_1^s+\varphi_2^s)|_{z=0}\\ +\frac{f^2}{2!}\frac{\partial}{\partial z}\frac{\partial}{\partial z}\left(\varphi_0^s+\varphi_i+\varphi_1^s\right)\Big|_{z=0}\\ +\frac{f^3}{3!}\frac{\partial}{\partial z}\frac{\partial}{\partial z}\frac{\partial}{\partial z}\left(\varphi_i+\varphi_0^s\right)\Big|_{z=0}\end{pmatrix}\exp(-ik\sin\theta_s x) \tag{17c}$$

$$\cdots$$

$$\begin{aligned}\varphi_n^{Ns}(\theta_s) \;=\; &\int_{-\frac{L}{2}}^{\frac{L}{2}} dx\begin{pmatrix}\varphi_i|_{z=0}+f\frac{\partial}{\partial z}\left(\varphi_i+\varphi_0^s+\varphi_1^s+\varphi_2^s+\cdots+\varphi_{n-1}^s\right)\big|_{z=0}\\ +\frac{f^2}{2!}\frac{\partial}{\partial z}\frac{\partial}{\partial z}\left(\varphi_0^s+\varphi_i+\varphi_1^s+\varphi_2^s+\cdots+\varphi_{n-2}^s\right)\Big|_{z=0}\\ +\frac{f^3}{3!}\frac{\partial}{\partial z}\frac{\partial}{\partial z}\frac{\partial}{\partial z}\left(\varphi_0^s+\varphi_i+\varphi_1^s+\varphi_2^s+\cdots+\varphi_{n-3}^s\right)\Big|_{z=0}\\ +\cdots+\frac{f^n}{n!}\underbrace{\frac{\partial}{\partial z}\frac{\partial}{\partial z}\cdots\frac{\partial}{\partial z}}_{n}\left(\varphi_i+\varphi_0^s\right)\Big|_{z=0}\end{pmatrix}\\ &\cdot\exp\left(-ik\sin\theta_s x\right)\end{aligned} \tag{17n}$$

where, L is the length of the finite rough surface. In this paper, the scattering coefficient is defined in this way [3], the integration of the scattering coefficient over the scattering angles upon the rough surface equals the ratio of the power received to that of scattered. Usually, for the infinite surface, a plane wave expressed like $\varphi_i = \exp(i\mathbf{k}\cdot\mathbf{r})$ is used as the incident wave. While, for the finite surface case discussed in this paper, a form of tapered plane wave expressed as following, is employed as the incidence field to avoid the 'edge diffraction effect' at the two edges of the surface [14]

$$\begin{aligned}\varphi_{inc}(\mathbf{r}) \;=\; &\exp(i\mathbf{k}\cdot\mathbf{r}(1+\left[2(x+z\tan\theta_i)^2/g^2-1\right]/(kg\cos\theta_i)^2))\\ &\cdot\exp(-(x+z\tan\theta_i)^2/g^2)\end{aligned} \tag{18}$$

where g denotes the tapered factor. Incident wave of this kind has power of $\mathbf{S}_{inc}\cdot\hat{z}$ per unit area, and $\mathbf{S}_{inc}$ is the Poynting vector of the

incident wave. Thus the power received by the finite rough surface of length L with plane wave incidence and tapered wave incidence, respectively, can be written as [14]

$$P_{inc}=-\int_{-L/2}^{L/2}dx\,(S_{inc}\cdot\hat{z})_{z=0}=-\int_{-l/2}^{L/2}dx\left(-\frac{1}{2\eta k}\mathrm{Im}\left(\varphi_i\frac{\partial}{\partial z}\varphi_i\right)\right)_{z=0}$$
$$=\begin{cases}-\frac{1}{2\eta k}\left(\int_{-L/2}^{L/2}dx\,(k\cos\theta_i\cos 2k(\sin\theta_i x-\cos\theta_i z))\right)\ (plane\ wave)\\ \frac{1}{2\eta k}\left(\int_{-L/2}^{L/2}dx(k\cos\theta_i)\left(1+\frac{2x^2/g^2-1}{(kg\cos\theta_i)^2}\right)-\frac{4k\sin\theta_i\tan\theta_i x^2}{k^2g^4\cos^2\theta_i}\right)\exp\left(-\frac{2x^2}{g^2}\right)\begin{pmatrix}tapered\\ wave\end{pmatrix}\end{cases} \tag{19}$$

where η is the intrinsic impedance of free space. Therefore, the expression for the normalized far-field bistatic scattering coefficient (BSC) is given as

$$\begin{aligned}\underset{\text{(plane wave)}}{\sigma_n(\theta_i,\theta_s)} &= \frac{r'S_s(r')}{-\int_{-L/2}^{L/2}dx(S_{inc}\cdot\hat{z})_{z=0}}\\ &= \frac{-\frac{1}{2\eta k}\mathrm{Im}(\varphi_n^s(r')\nabla\varphi_n^{s*}(r'))}{-\frac{1}{2\eta k}(\int_{-L/2}^{L/2}dx(k\cos\theta_i\cos 2k(\sin\theta_i x-\cos\theta_i z)))}\\ &= \frac{(k\cos\theta_s)^2|\varphi_n^{Ns}(\theta_s)|^2}{2\pi\int_{-L/2}^{L/2}dx(k\cos\theta_i(2k(\sin\theta_i x-\cos\theta_i z)))}\end{aligned} \tag{20}$$

$$\begin{aligned}\underset{\text{(tapered wave)}}{\sigma_n(\theta_i,\theta_s)} &= \frac{r'S_s(r')}{-\int_{-L/2}^{L/2}dx\,(S_{inc}\cdot\hat{z})_{z=0}}\\ &= \frac{-\frac{1}{2\eta k}\mathrm{Im}\left(\varphi_n^s(r')\nabla\varphi_n^{s*}(r')\right)}{-\frac{1}{2\eta k}\begin{pmatrix}\int_{-L/2}^{L/2}dx(k\cos\theta_i)\left(1+\frac{2x^2/g^2-1}{(kg\cos\theta_i)^2}\right)\\ -\frac{4k\sin\theta_i\tan\theta_i x^2}{k^2g^4\cos^2\theta_i}\end{pmatrix}\exp\left(-\frac{2x^2}{g^2}\right)}\\ &= \frac{(k\cos\theta_s)^2\left|\varphi_n^{Ns}(\theta_s)\right|^2}{2\pi\left(\int_{-L/2}^{L/2}dx(k\cos\theta_i)\left(1+\frac{2x^2/g^2-1}{(kg\cos\theta_i)^2}\right)-\frac{4k\sin\theta_i\tan\theta_i x^2}{k^2g^4\cos^2\theta_i}\right)\exp\left(-\frac{2x^2}{g^2}\right)}\end{aligned} \tag{21}$$

where $\varphi_n^{Ns}(\theta_s)$ can be found in (17a)–(17n) with the incident wave of tapered wave. The expressions for the first- to third- order scattering coefficients of the classical SPM are given in [3, 26] Considering the rough surface studied by the classical SPM is infinite extent, a plane wave expressed as $\varphi_i=\exp(i\mathbf{k}\cdot\mathbf{r})$ is used in the classical SPM, and the advantage of the integral SPM with tapered wave incidence avoids the

diffraction effect at edge of the surface effectively will be investigated in the numerical section.

4. NUMERICAL RESULTS

Several numerical examples are carried out in this Section to evaluate the validation and efficiency of the above presented method in detail. As the MOM has been proved to be accurate in a great degree for modeling EM scattering from rough surface by many works [14], it is used in this Section to test the accuracy of higher order integral SPM. In Fig. 2, Fig. 3 and Fig. 5 Gaussian spectral density function [3] is employed to test the validity of our theory in an easy way, and in Fig. 4 and Fig. 6 the PM spectrum [14] is applied to extend our theory. In Fig. 2(a)–Fig. 2(c), 'p.w.f', 't.w.f' and 'p.w.i' denote 'plane wave incident on finite surface', 'tapered plane wave incident on finite plane' and 'plane wave incident on infinite surface', respectively. In Fig. 3–Fig. 6, 'integral SPM' is for 'tapered wave incident on finite surface', 'classical SPM' is for 'plane wave incident on infinite surface', and 'MOM' is for 'tapered wave incident on finite surface'.

Figures 2(a)–(c) present the comparison between the integral SPM and the classical SPM from the first-order to the third-order with the incident wavelength 0.45 cm the correlation length $l = 0.427\lambda$, and the rms height $h = 0.105\lambda$. The rough surface is divided into 1024 segments (1024 pts shown in the figure), the length of the surface is 100λ, the tapered factor g is $L/4.2$ (L represents the length of the rough surface) [14]. Considering the random quality of rough surface studied in this paper, results for 5 surface realizations are achieved and averaged. It is shown that, for the finite surface, the bistatic scattering coefficient by the integral SPM with plane wave incidence is higher than that by the integral SPM with tapered wave incidence, no matter which order integral SPM is used. However, good agreement of the bistatic scattering coefficients can be observed between the integral SPM (for finite surface with tapered wave incidence) and the classical SPM (for infinite surface with plane wave incidence) for different order integral SPM. Based on the above illustrations and comparisons, we can conclude that the results are not accurate when the plane wave is still applied when the infinite surface is truncated into a finite one (as it can generate the so called 'edge diffraction effect' on the two ends of the finite surface). While the 'edge diffraction effect' can be greatly avoided by the integral SPM with tapered wave incidence. It can also be found that, a peak with finite angular width can be found within the integral SPM in the specular direction, and this is due to the coherent scattering by the finite surface. While the incoherent scattering is just

included in the expression of the classical SPM (p.w.i), and no peak is shown in the specular direction. It should be mentioned that the amplitude of the fluctuations in the curves is due to the Monte-Carlo procedure used to render the surfaces.

In order to further examine the validity of the integral SPM for the surface with Gaussian spectrum, Fig. 3(a)–Fig. 3(c) gives the comparison of BSC between the integral SPM and the MOM [14], where the results for 20 surface realizations are averaged and the result by MOM is considered to be an accurate one in a great extent By comparing the scattering pattern of ISPM with that of MOM, it is observed that only for the first-order integral SPM do we have a visible discrepancy between the plots by ISPM and MOM in Fig. 3(a), the more pronounced departure appears at scattering region of $-90° \sim 0°$. It is indicated that, the low order ISPM is not exact enough in this case,

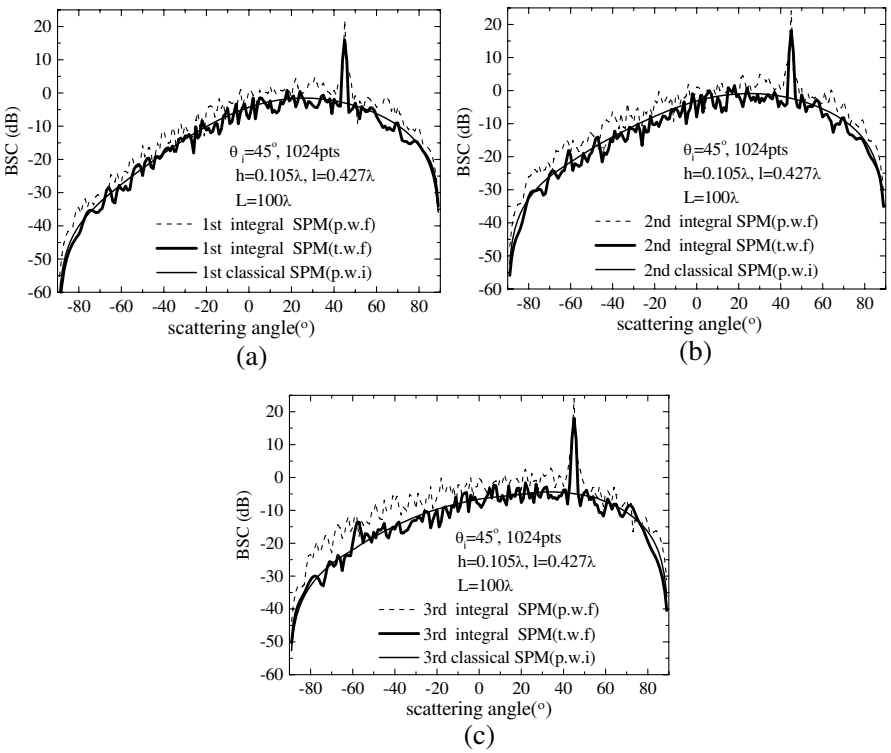

Figure 2. (a) 1st classical SPM and 1st integral SPM. (b) 2nd classical SPM and 2nd integral SPM. (c) 3rd classical SPM and 3rd integral SPM.

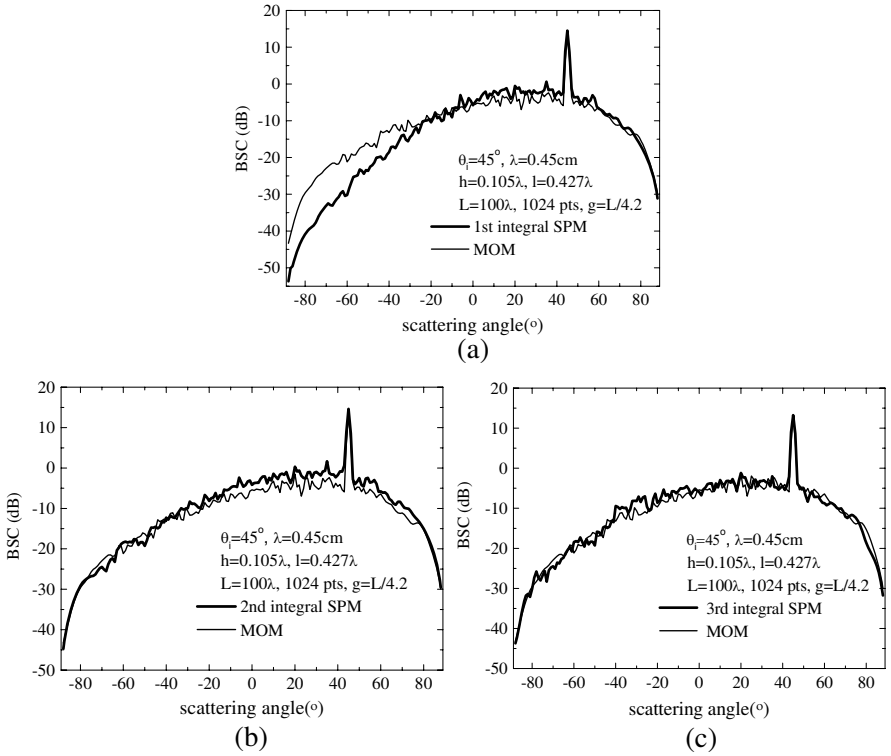

Figure 3. (a) 1st integral SPM and MOM. (b) 2nd integral SPM and MOM. (c) 3rd integral SPM and MOM.

and the higher order item should be considered for the more exactness. As for the second-order ISPM to the third-order ISPM is concerned, it is shown that the higher order ISPM, the better agreement between BSC of ISPM and MOM.

The validity of integral SPM is also presented in Fig. 4 for the conducting gentle rough ocean surface with PM ocean spectrum [14], where the results for 10 rough surface realizations are averaged. Fig. 4 shows the comparison of the first-order and third-order ISPM calculations with MOM calculations for the angular distribution of BSC. It is also obvious that the two methods are in fairly good agreement over all scattering angles for the slightly sea surface scattering with low wind speed (denoted by u in the figure).

To further evaluate the efficiency of the presented method, Table 1 and Table 2 show the comparisons between the third-order ISPM and MOM in memory requirements and average computational time for the

Table 1. The comparison of the third-order ISPM and MOM in memory and time (Gaussian Spectrum).

Size of Surface (ISPM MOM)	Number of Segments (ISPM, MOM)	Memory Requirements (ISPM/MOM)	Computational Time (ISPM/MOM)
25.6λ	256	1.363 MB/3.172 MB	3s/3s
51.2λ	512	1.445 MB/9.203 MB	7s/50s
100λ	1024	1.641 MB/32.676 MB	15s/6m 18s
200λ	2048	1.992 MB/64.211 MB	31s/1h1m16s

Table 2. The comparison of the third-order ISPM and MOM in memory and time (PM Spectrum).

Size of Surface (ISPM, MOM)	Number of Segments (ISPM, MOM)	Memory Requirements (ISPM/MOM)	Computational Time (ISPM/MOM)
25.6λ	256	1.359 MB/3.168 MB	3s/3s
51.2λ	512	1.438 MB/8.598 MB	7s/52s
100λ	1024	1.641 MB/32.688 MB	15s/6m33s
200λ	2048	1.984 MB/65.328 MB	30s/1h1m32s

Gaussian spectrum and PM ocean spectrum, respectively. Except for the length of rough surface and the divided segments, other parameters of Table 1 correspond to those in Fig. 3(c) and parameters of Table 2 correspond to those in the Fig. 4. Results for 100 surface realizations are averaged. Both ISPM and MOM algorithms are tested on the PC with a 2.33 GHz processor (Intel Core 2 Quad Q8200), 4 GB Memory, and Fortran PowerStation 4.0 compiler. It can be found that, for the small size rough surface (25.6λ), the differences between the presented ISPM and MOM in memory requirements and computation time are not so obvious, but with the increasing of the surface size, the above mentioned differences is visually large. Also, the larger the rough surface size, the advantage of ISPM in memory requirements and computation time is more evident.

In Fig. 5 and Fig. 6, the bistatic scattering coefficients with low grazing angle incidence for Gaussian and PM spectrum surface are depicted, respectively. All the parameters are given in the figures. Ten surfaces realizations are averaged. In Fig. 5, the results for different rms height are investigated, and the third-order integral SPM is applied. It can be found that with the increasing of the rms height, the backward incoherent scattering increases, as the surface becomes

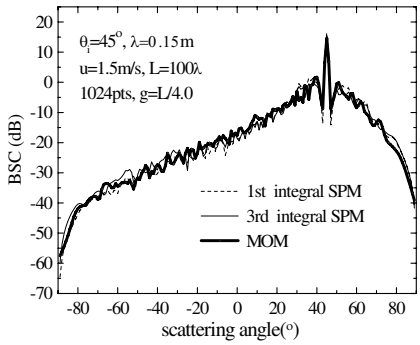

Figure 4. Scattering coefficient for PM ocean spectrum.

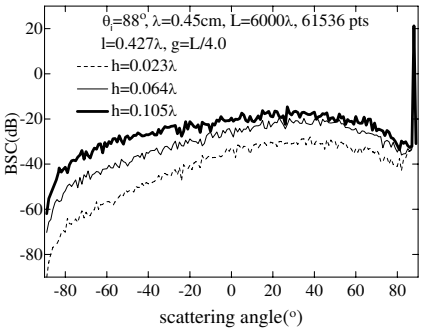

Figure 5. Low grazing angle incidence for Gaussian surface.

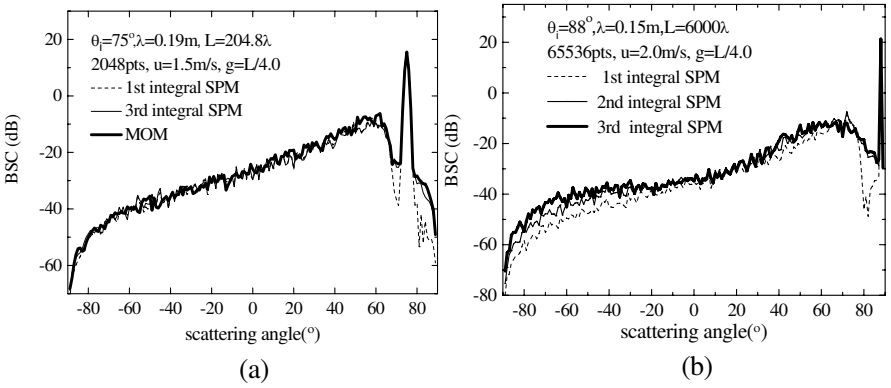

Figure 6. Large angle incidence for PM ocean surface.

rougher. It is worth noting that the results of the MOM are not presented here, due to the fact that, in these cases, the algorithm of MOM can not be performed, as the computational cost exceeds the maximal default memory requirement of the Fortran computational software.

In Fig. 6(a), the comparison of BSC by the integral SPM and MOM with large incident angle is also given. It is indicated that, the result of the third-order integral SPM is more exact than that of the first-order. In Fig. 6(b), when the size of the rough surface is large, the results for the first- to the third-order ISPM also show different accuracy. In both cases, the specular peak can be obtained. In Fig. 6(a), the computational time by the ISPM is 31 s, by the MOM is 1 h 3 m 12 s, the memory requirements by the ISPM is 1.984 MB, by the MOM is 65.328 MB. In Fig. 6(b), the curves by the MOM are

not plotted, because the algorithm of MOM can not be performed at these situations, the same reason discussed in Fig. 5. Therefore, the work of computing the large size rough surface under low incident angle, which can not be easily accomplished by the MOM due to its disadvantage of large memory dependence and time-consuming, but can be performed accurately and efficiently by the ISPM. That is mainly owing to its advantages of very low memory requirement and very high computation efficiency, and this is one of the main intention and significance of our work discussed in this paper. It should be noted that, in Figs. 4 and 5, the angular spectrum is qualitatively different for the case of ocean scattering (Fig. 4) and the Gaussian surface (Fig. 5), some information of the surface itself, such as parameters h, l, spectral density function $W(k)$, or wind speed u, etc., can be retrieved from the angular spectrum data, and this is related with the topic of inverse problem, which is valuable and worthy of further research.

5. CONCLUSIONS

In this paper, a high order integral SPM (HISPM) for rough surface scattering with tapered wave incidence is presented. The shortage of failure to compute the finite size rough surface by the classical SPM has been solved by the presented integral SPM. Both the incoherent and coherent scattering components are included within this method. The validity of this method is evaluated by comparing with the MOM. Only the first- to the third-order scattering coefficients are given in the classical SPM, while through the series expansion of the scattered wave, high order scattering coefficient can be obtained within this integral SPM. The scattering coefficients with low grazing angle incidence can also be calculated by this method, which have not ever be resolved in the previous papers about the SPM, to our knowledge. Results that should be ideal in a certain extent can be obtained through calculating higher order scattering coefficient by this method, when exact result can not be provided by the low order SPM. Unlike the classical SPM, the scheme presented in this paper is not confined by the surface spectral density function, it can also be widely applied to calculate the scattering coefficients of the slightly rough surface with obtaining the information of the height profile. The presented HISPM is intermediate in some respects between the analytical and the numerical methods ('semi-analytical' or 'semi-numerical'), but comparing with the analytical method-CSPM, it can improve the exactness, and comparing with the numerical method-MOM, it can decrease the memory requirement and increase computation efficiency, theses investigation or comparison also have not ever been carried out

in the previous work about the SPM to our knowledge. It should be pointed out that for the case of the transverse magnetic wave incidence (TM case), the derivation and the numerical simulations is under investigation, which will appear in our future paper, the numerical results presented in this paper also needs further verification by the relevant experiments.

ACKNOWLEDGMENT

This work was supported by the National Natural Science Foundation of China (Grant No. 60971067) and by the Fundamental Research Funds for the Central Universities. The authors would like to thank the reviewers for their constructive suggestions.

REFERENCES

1. Rice, S. O., *Reflection of Electromagnetic Waves from Slightly Rough Surfaces, in Theory of Electromagnetic Waves*, Wiley, New York, 1951.
2. Lin. Z. W, X. J. Zhang, and G. Y. Fang, "Theoretical model of electromagnetic scattering from 3D multi-layer dielectric media with slightly rough surfaces," *Progress In Electromagnetics Research*, Vol. 96, 37–62, 2009.
3. Tsang, L. and J. A. Kong, *Reflection of Electromagnetic Waves from Slightly Rough Surfaces, in Theory of Electromagnetic Waves*, Wiley, New York, 2000.
4. Johnson, J. T., "Third-order small-perturbation method for scattering from dielectric rough surfaces," *J. Opt. Soc. Am. A.*, Vol. 16, No. 11, 2720–2736, 1999.
5. Wu. Z.-S, J.-J. Zhang, and L. Zhao, "Composite electromagnetic scattering from the plate target above a one-dimensional sea surface: Taking the diffraction into account," *Progress In Electromagnetics Research*, Vol. 92, 317–331, 2009.
6. Ishimaru, A., C. Le, Y. Kuga, L. A. Sengers, and T. K. Chan, "Polarimetric scattering theory for high slope rough surface," *Progress In Electromagnetics Research*, Vol. 14, 1–36, 1996.
7. Beckman, P. and A. Spizzichino, *The Scattering of Electromagnetic Waves from Rough Surfaces*, Pergamon, Oxford, 1963.
8. Johnson, J. T., R. T. Shin, and K. Pak, "A numerical study of the composite surface model for ocean backscattering," *IEEE Trans.Geosci. Remote Sensing*, Vol. 36, No. 1 72–83, 1998

9. Winebrenner, D. P., and A. Ishimaru, "Application of the phase-perturbation technique to randomly rough surfaces," *J. Opt. Soc. Am. A.*, Vol. 2, No. 12, 2285–2294, 1985.
10. Baudier, C. and R. Dusséaux, "Scattering of an E||-polarized plane wave by one-dimensional rough surfaces: Numerical applicability domain of a Rayleigh method in the far-field zone," *Progress In Electromagnetics Research*, Vol. 34, 1–27, 2001.
11. Guo, L. X. and Z. S. Wu, "Application of the extended boundary condition method to electromagnetic scattering from rough dielectric fractal sea surface," *Journal of Electromagnetic Waves and Applications*, Vol. 18, No. 9, 1219–1234, 2004.
12. Liang. D, P. Xu, L. Tsang, Z. Gui, and K.-S. Chen, "Electromagnetic scattering by rough surfaces with large heights and slopes with applications to microwave remote sensing of rough surface over layered media," *Progress In Electromagnetics Research*, Vol. 95, 199–218, 2009.
13. Dusséaux, R. and R. de Oliveira, "Scattering of a plane wave by a 1-dimensional rough surface study in a nonorthogonal coordinate system," *Progress In Electromagnetics Research*, Vol. 34, 63–88, 2001.
14. Tsang, L. and J. A. Kong, *Scattering of Electromagnetic Waves — Numerical Simulations*, Wiley, New York, 2000.
15. Wang, A. Q., L. X. Guo, and C. Cai, "Numerical simulations of electromagnetic scattering from 2D rough surface: Geometric modeling by NURBS surface," *Journal of Electromagnetic Waves and Applications*, Vol. 24, No. 10, 1315–1328, 2010.
16. Chan, C. H., S. H. Lou, L. Tsang, and J. A. Kong, "Electromagnetic scattering of waves by random rough surface: A finite-difference time-domain approach," *Microwave Opt. Technol. Lett.*, Vol. 4, No. 9, 355–359, 1991.
17. Li, J., L. X. Guo, and H. Zeng, "FDTD method investigation on the polar-metric scattering from 2-D rough surface," *Progress In Electromagnetics Research*, Vol. 101, 173–188, 2010.
18. Li, J. and L. X. Guo, "Message-passing-interface-based parallel FDTD investigation on the EM scattering from a 1-D rough sea surface using uniaxial perfectly matched layer absorbing boundary," *J. Opt. Soc. Am. A.*, Vol. 26, No. 6, 1494–1502, 2009.
19. Lou, S., H., L. Tsang, and C. H. Chan, "Application of finite element method to Monte Carlo simulations of scattering of waves by random rough surfaces: Penetrable case," *Waves in Random Media*, Vol. 1, No. 4, 287–307, 1991.

20. Jandhyala, V., E. Michielssen, S. Balasubramaniam, and W. C. Chew, "A combined steepest descent-fast multipole algorithm for the fast analysis of three-dimensional scattering by rough surfaces," *IEEE Trans. Geosci. Remote Sensing*, Vol. 36, No. 3, 738–748, 1998.
21. Liang, Y., L. X. Guo, and Z. S. Wu, "The EPILE combined with the Generalized-FBM for analyzing the scattering from targets above and on a rough surface," *IEEE Antennas Wireless Propag. Lett.*, Vol. 9, 809–813, 2010.
22. Li, S. Q., C. H. Chan, L. Tsang, and Q. Li, "Parallel implementation of the sparse matrix/canonical grid method for the analysis of two-dimensional random rough surfaces (three-dimensional scattering problem) on a Beowulf system," *IEEE Trans. Geosci. Remote Sensing*, Vol. 38, No. 4, 1600–1608, 2000.
23. Bass, F. G. and I. M. Fuks, *Wave Scattering from Statistically Rough Surfaces*, Pergamon, Oxford, 1979.
24. Thorsos, E. and D. R. Jackson "The validity of the perturbation approximation for rough surface scattering using a Gaussian roughness spectrum," *J. Acoust. Soc. Am.*, Vol. 86, No. 1, 261–277, 1989.
25. Soto-Crespo, J. M., M. Nieto-Vesperinas, and A. T. Friberg, "Scattering from slightly rough random surfaces: A detailed study on the validity of the small perturbation method," *J. Opt. Soc. Am. A.*, Vol. 7, No. 7, 1185–1201, 1990.
26. Kim, M. J. and A. J. Stoddart, "The region of validity of perturbation theory," *Waves in Random Media*, Vol. 3, No. 4, 325–342, 1993.
27. Ishimaru, A., J. D. Rockway, and Y. Kuga, "Rough surface Green's function based on the first-order modified perturbation and smoothed diagram methods," *Waves in Random Media*, Vol. 10, No. 1, 17–31, 2000.
28. Guérin, C. A. and A. Sentenac, "Second-order perturbation theory for scattering from heterogeneous rough surfaces," *J. Opt. Soc. Am. A.*, Vol. 21, No. 7, 1251–1260, 2004.
29. Brelet, Y. and C. Bourlier, "Spm numerical results from an effective surface impedance for a one-dimensional perfectly-conducting rough sea surface," *Progress In Electromagnetics Research*, Vol. 81, 413–436, 2008.
30. Pattanayak, D. N. and E. Wolf, "General form and a new interpretation of the Ewald-Oseen extinction theorem," *Optics Communications*, Vol. 6, No. 3, 217–220, 1972.